INVESTIGATION OF THE TIME DEPENDENT MECHANICAL PROPERTIES DUE TO ELASTIN DEGRADATION IN PORCINE MITRAL VALVE ANTERIOR LEAFLETS

By

Shubhra Singhal

A capstone project submitted for Graduation with University Honors

May 7, 2026

University Honors

University of California, Riverside

APPROVED

Dr. Chung-Hao Lee

Department of Bioengineering

Dr. Begoña Echeverria, Howard H Hays, Jr. Chair

University Honors

ABSTRACT

Mitral valve degeneration is a common age-related condition that progressively impairs cardiac function by reducing the flexibility and structural integrity of the valve leaflets. The mitral valve regulates blood flow from the left atrium to the left ventricle, and its dysfunction can lead to regurgitation, a condition in which the valve fails to close fully and allows backward flow into the atrium. A key contributor to this degeneration is the gradual breakdown of elastin, an extracellular matrix (ECM) protein that enables the valve leaflets to stretch and recoil during each heartbeat. As elastin deteriorates, mechanical loading shifts to stiffer collagen fibers, which can alter leaflet motion and contribute to disorders such as mitral valve prolapse. Previous research has characterized tissue behavior after complete or nearly complete removal of elastin, but aging occurs as a gradual process rather than an abrupt loss of the ECM components. As a result, little is known about how progressive elastin degradation affects the mechanical properties of mitral valve tissue over time. This project addresses this gap by quantifying tissue-level mechanical changes in porcine mitral valve anterior leaflets following controlled, stepwise degradation of elastin. The study employs three methods: *(i)* biaxial tension and stress-relaxation testing of untreated leaflet samples to establish baseline properties, *(ii)* enzymatic treatment at defined time intervals to selectively degrade elastin, and *(iii)* repeated biaxial mechanical testing after each degradation stage. By correlating changes in mechanical response with the time course of elastin loss, this work aims to clarify how aging-like ECM remodeling alters valve function. These findings are expected to improve understanding of how degenerative processes develop and may ultimately inform more effective surgical repair strategies and computational models of valve mechanics.

ACKNOWLEDGMENTS

I gratefully acknowledge the Bioengineering Biomechanics and Design Laboratory (BBDL) in the Department of Bioengineering at UCR for their continuous support, collaboration, and contributions throughout the duration of this project. The environment fostered within the lab played a central role in shaping both the scientific direction and the quality of this work. I extend my sincere appreciation to Dr. Chung-Hao Lee for his guidance, insight, and leadership. His mentorship not only strengthened the technical rigor of this study but also encouraged my growth as an independent researcher. I would also like to thank the Ph.D. students in the BBDL for their dedication, expertise, and the many valuable discussions that helped refine the experimental design, data interpretation, and overall scientific approach. Their willingness to share knowledge and provide thoughtful feedback was instrumental to the success of this work. Finally, I acknowledge my fellow undergraduate researchers for their hard work, teamwork, and commitment during data collection, sample preparation, and experimental procedures. Their support and collaboration made the research process both productive and rewarding. I am deeply appreciative of the collective effort that contributed to the completion of this project.

TABLE OF CONTENTS

INTRODUCTION

Heart Anatomy and its Role in Circulation

The heart is a muscular organ located in the center of the chest with a slight shift toward the left side. It acts as the main pump that drives blood circulation and supports the continuous delivery of oxygen and nutrients throughout the body. Structurally, it is divided into four chambers: the right atrium, right ventricle, left atrium, and left ventricle. The upper chambers called the atria receive incoming blood, while the lower chambers, called the ventricles, generate the force needed to push blood forward (Rehman, 2023).

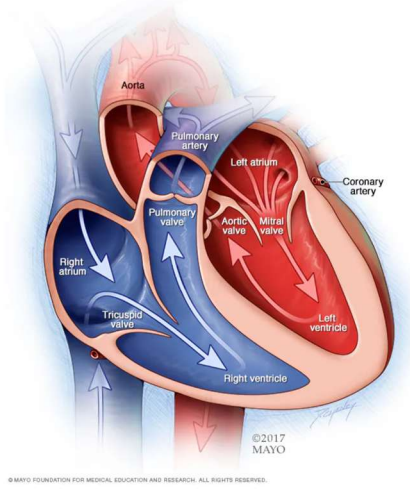

Figure 1: *Image of the anatomy of the heart from Mayo Clinic.*

The right side of the heart is responsible for handling deoxygenated blood returning from the body. Blood enters the right atrium, moves through the tricuspid valve into the right ventricle, and is then pumped to the lungs through the pulmonary artery (Figure 1). In the lungs, gas exchange occurs, where carbon dioxide is released and oxygen is absorbed. The oxygenated blood then returns to the heart through the pulmonary veins and enters the left atrium.

From there, blood flows into the left ventricle through the mitral valve. The left ventricle has a much thicker muscular wall because it must generate enough pressure to send blood through the entire body. When it contracts, blood is pushed through the aortic valve into the aorta and distributed to tissues and organs (Figure 1). This cycle repeats continuously with every heartbeat.

The heart valves, including the tricuspid, pulmonary, mitral, and aortic valves, are essential for maintaining this flow. They ensure that blood moves in only one direction by preventing

backflow during each phase of the cardiac cycle, allowing the heart to function efficiently as a coordinated pump.

The Mitral Valve

The mitral valve is a gate-like structure in the heart that connects the left atrium to the left ventricle on the left side of the cardiac system. It is responsible for regulating the passage of blood between these two chambers, and it maintains a unidirectional flow of blood for the heart to function properly. The valve is composed of two leaflets that operate together to open during ventricular filling and close during ventricular contraction so that blood continues to move forward without leaking backward (Figure 2).

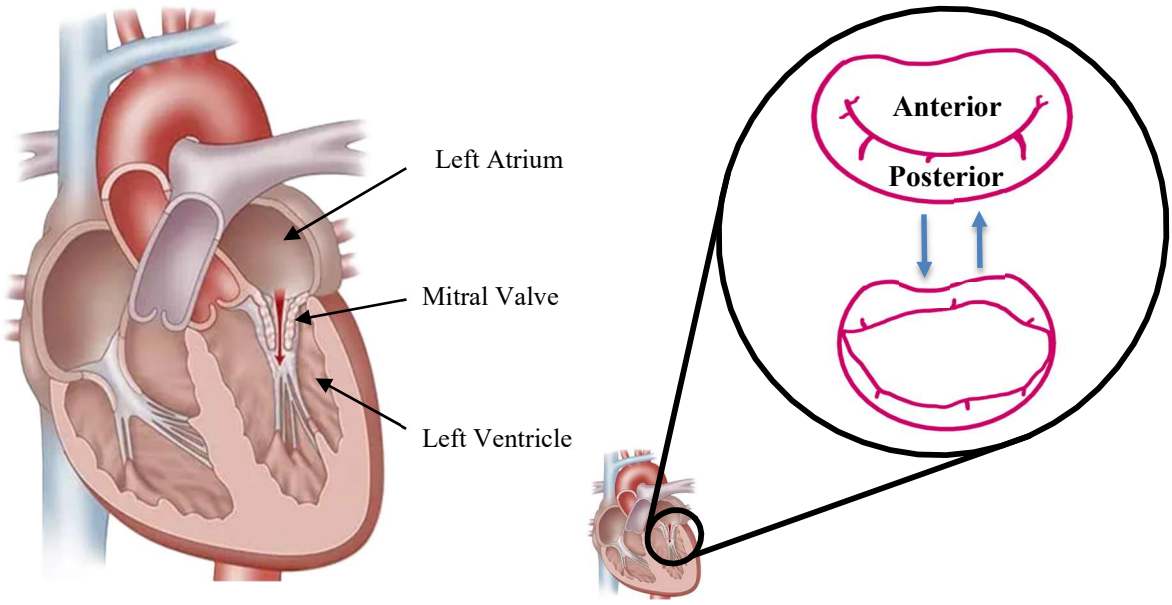

Figure 2: *Anatomy of the mitral valve from Heart360Care, showing its position between the left atrium and left ventricle and a magnified view of the anterior and posterior leaflets.*

The two leaflets are known as the mitral valve anterior leaflet (MVAL), which is positioned toward the front of the heart, and the mitral valve posterior leaflet (MVPL), which sits behind it

(Ross *et al.*, 2021). They work in coordination to preserve efficient and controlled blood flow from the left atrium into the left ventricle.

The two mitral valve leaflets are supported by a highly organized network of structural proteins collectively known as the extracellular matrix, or ECM (Kodigepalli *et al*, 2020). This matrix provides the leaflet with the mechanical characteristics required for its role including strength, flexibility, and the ability to withstand repeated loading. The ECM is composed of three major constituents that each contribute to the overall behavior of the tissue (Figure 3). Collagen fibers form the primary load bearing framework. Elastin fibers supply elasticity and allow the leaflet to stretch and then recoil so the leaflet tissue can return to its original geometry after deformation. Glycosaminoglycans, often referred to as GAGs, mediate between collagen and elastin. They help regulate interactions between the two fiber systems and promote cross-linking that stabilizes the matrix (Ross *et al*, 2021). Together, these components create a complex and dynamic structure that enables the mitral valve to perform its biomechanical function throughout continuous cycles of opening and closing.

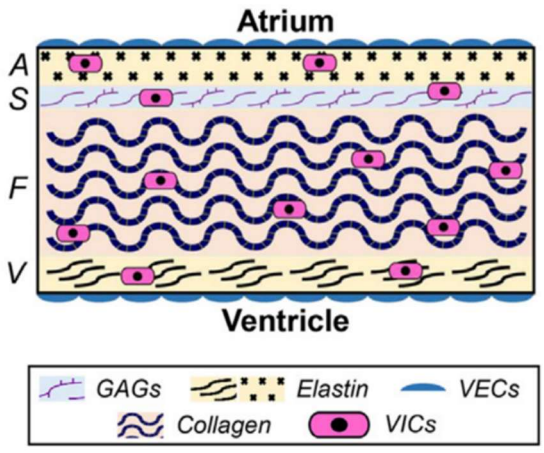

Extracellular Matrix (ECM) Components:

- Collagen for Load Bearing
- Elastin for Elasticity and Flexibility
- GAGs for Bridging Collagen and Elastin
- VECs for Controlling Cell Activation
- VICs for Regulating Tissue Remodeling

Figure 3: *Extracellular matrix structure of the mitral valve from Ross et al. (2021), showing the four layers and distribution of collagen, elastin, GAGs, VECs, and VICs.*

Elastin Degradation

Aging-related cardiovascular diseases present a significant global healthcare challenge, with valvular dysfunction contributing to high mortality and reduced quality of life among older populations. Aging is not a single change, but a complex process characterized by the gradual decline of function. Mitral valve disease, which affects approximately 7.5% of adults over 75 years old (Carrabba *et al*, 2025), develops because of progressive structural changes that interfere with the valve's ability to regulate blood flow effectively between the left atrium and left ventricle. As described earlier, proper mitral valve function depends on the integrity of the extracellular matrix, where collagen, elastin, and GAGs interact to maintain mechanical balance, strength, and flexibility.

With age in some cases, elastin fibers experience remodeling and fragmentation, processes that weaken their flexibility and reduce their ability to contribute to tissue elasticity (Figure 4). Multiple factors contribute to this deterioration, including repeated mechanical stress that can induce microfractures, as well as biochemical modifications such as calcification, and oxidative reactions (Duca *et al*, 2016). These mechanisms collectively increase the susceptibility of elastin to damage and fragmentation, increasing its loss of function within the extracellular matrix. This leads to a redistribution of mechanical loads toward collagen fibers, which are substantially stiffer than elastin and dominate the mechanical response under these conditions. As elastin degrades and collagen becomes more dominant, the valve tissue exhibits reduced compliance and increased stiffness, limiting the leaflet's ability to recoil and return to its original configuration (Duca *et al*, 2016).

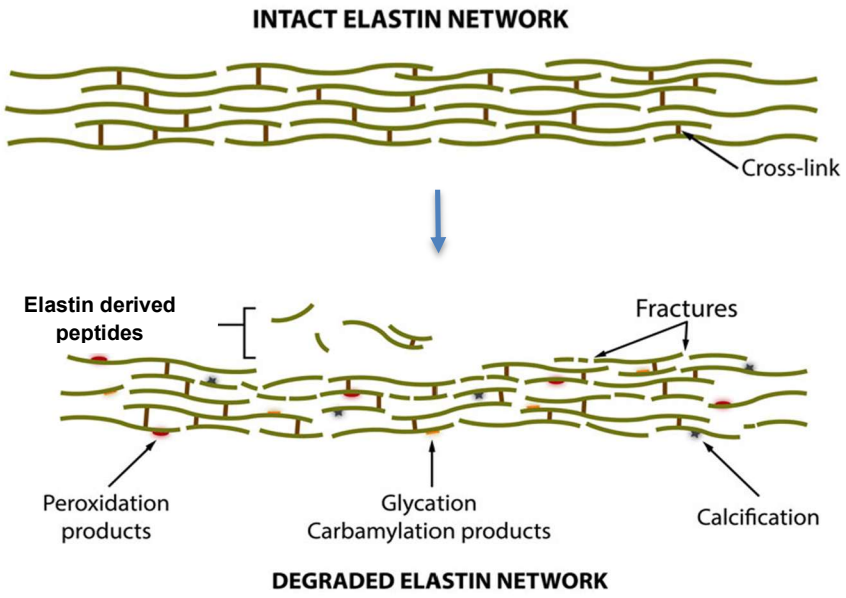

Figure 4: *Intact versus degraded elastin networks from Duca et al (2016), highlighting fiber fragmentation and associated biochemical degradation products.*

This progression in material properties interferes with the valve's ability to maintain proper closure and can contribute to the development of conditions such as mitral valve prolapse, where incomplete leaflet coaptation disrupts efficient blood flow, reduces left ventricular ejection fraction, and increases the risk of further complications (Figure 5). To better understand the contribution of elastin to mitral valve biomechanics, researchers conducted artificial enzymatic degradation on MVALs to selectively remove elastin from valve tissue and evaluate the resulting mechanical changes. By comparing treated samples with untreated controls, these studies have demonstrated that elastin contributes to both low and high

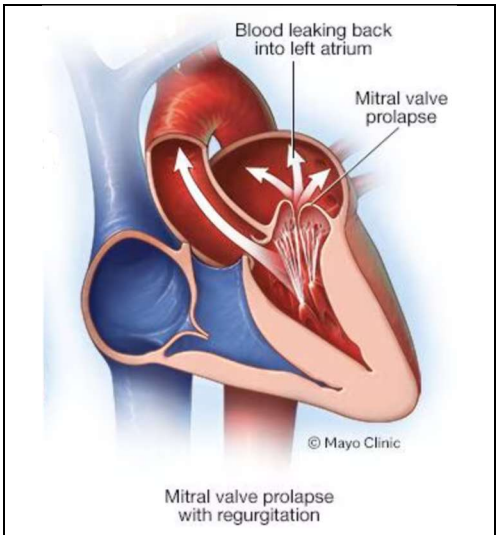

Figure 5: *Depiction of Mitral Valve Prolapse from Mayo Clinic.*

stress mechanical behavior, while collagen primarily supports load bearing under higher tension. Despite these findings, prior work has largely focused on complete removal of elastin, leaving a gap in understanding how gradual or partial loss of elastin influences tissue mechanics (Ross *et al*, 2021). To address this limitation, the present project investigates the time dependent effects associated with progressive enzymatic degradation of elastin within MVAL. By introducing controlled, incremental reductions in elastin content, this approach allows for a more detailed examination of how changes in elastin levels changes mechanical properties over time, providing insight into how the interaction between elastin and collagen evolves as degradation progresses and how these changes influence overall valve function. Through this analysis, the role of elastin in maintaining valve mechanics as well as its contribution to age related dysfunction becomes more defined, with findings that may inform improvements in surgical interventions such as annuloplasty through a refined understanding of valve tissue behavior.

METHODS

Previous studies investigating mitral valve biomechanics have demonstrated that elastin plays an essential role in regulating tissue flexibility, particularly in the radial direction of the MVAL. Through enzymatic treatments to selectively remove elastin, previous researchers have shown that degradation occurs rapidly, with histological evidence indicating that complete elastin loss is achieved within approximately 15 minutes of treatment (Ross *et al*, 2021). Following this degradation, clear structural and mechanical changes are observed within the tissue. Under normal conditions, intact valve leaflets exhibit greater radial stretch than circumferential stretch, a behavior that is largely attributed to the presence and functional contribution of elastin fibers (Ross *et al*, 2021). However, once elastin is fully degraded, radial extensibility is significantly reduced, indicating a shift in mechanical load bearing toward the stiffer collagen network (Figure 6).

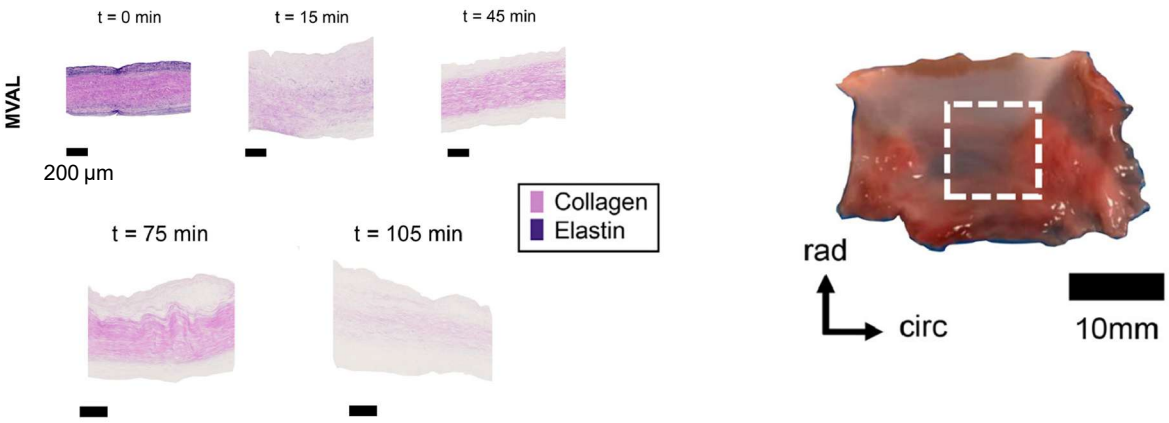

Figure 6: *Histological images of the MVAL (left) from Ross et al (2021), showing collagen (pink) and elastin (dark purple) distribution at 0, 15, 45, 75, and 105 minutes. The right panel shows the tissue sample with radial and circumferential orientations.*

While these findings highlight the importance of elastin in maintaining normal mitral valve mechanics, they are primarily based on conditions of complete elastin removal. As a result, there remains a gap in understanding how incremental, time-dependent changes in elastin content influence the mechanical behavior of valve tissue. The goal of this study is to address this limitation by investigating how mitral valve mechanics evolve during progressive elastin degradation within the 15-minute enzymatic window. By examining tissue behavior at multiple intermediate time points leading up to complete elastin loss, this work aims to provide a more detailed and physiologically relevant understanding of how gradual elastin breakdown affects the interaction between elastin and collagen and, in turn, alters overall valve function.

Tissue Preparation

Adult porcine hearts were collected from a local slaughterhouse and were rinsed thoroughly to remove any remaining blood and debris. After cleaning, the hearts were stored at −20 °C until they were needed for experiments. On the day of use, each heart was thawed at 4 °C so the tissue could be handled without damaging the leaflet structure. Once thawed, the mitral

valve was dissected, and the anterior leaflet was isolated for enzymatic treatment for histology procedures and biaxial testing described in the following sections.

Histology for Tissue ECM Constituent Quantification

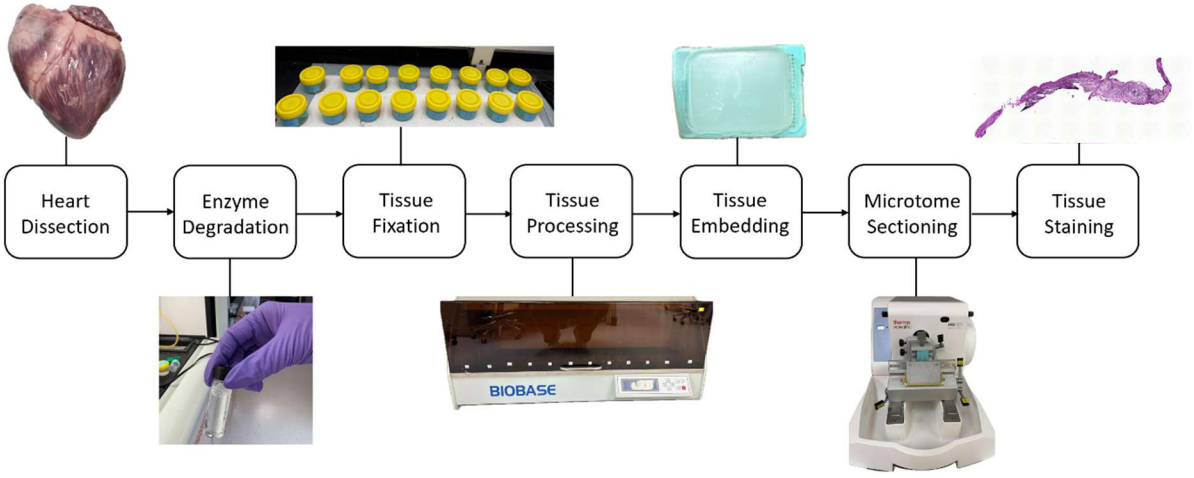

Figure 7: *Workflow for histological preparation of valve tissue, from dissection through staining.*

Adult porcine hearts were obtained and used as the source of mitral valve tissue due to their structural similarity to human cardiac anatomy. After initial dissection, the MVAL was isolated and trimmed to remove excess chordal tissue. The leaflet was then sectioned into sixteen thin, uniform strips cut specifically along the circumferential direction to maintain consistent fiber orientation across all samples. One strip served as the untreated control, while the remaining fifteen strips were assigned to incremental elastase treatment times ranging from 1 to 15 minutes. Each strip was submerged in an elastase solution composed of phosphate-buffered saline (PBS), 60 units/mL elastase, and 0.1 mg/mL trypsin inhibitor (Figure 7). This mixture allowed controlled, time-dependent degradation of elastin while limiting nonspecific activity. Each strip remained in the solution for its designated duration to produce a progressive series of reduced elastin samples.

Immediately after treatment, all tissue strips were rinsed with 4 °C PBS and placed into 10% neutral buffered formalin to halt enzymatic activity and preserve extracellular matrix architecture for histological evaluation (Figure 7). Following fixation, samples were processed in an automated tissue processor, where they were cleared, and infiltrated with molten paraffin wax. This process replaced water within the tissue with paraffin, providing the rigidity required for precise microtome sectioning.

Each strip was then embedded individually into paraffin blocks and oriented to allow consistent sectioning across all samples (Figure 7). Using a microtome, the embedded tissues were cut into 7-micrometer-thick sections and mounted onto charged glass slides to ensure strong adhesion during staining. Prepared slides were submitted for Verhoeff–van Gieson (VVG) staining, which stains elastin fibers black and collagen pink, allowing clear visualization of elastin content across the progressive treatment times. Stained slides were imaged and quantified using the Keyence BZ-X800 microscope. Elastin content was measured by calculating the pixel content of black-stained regions relative to total tissue area. These values were used to generate a percent elastin reduction curve as a function of treatment time. The resulting plot demonstrated rapid elastin loss during the early minutes of treatment, followed by a plateau indicating near-complete degradation at approximately **9 minutes** (Figure 8). In addition to the quantitative curve, visual inspection of the VVG-stained sections revealed that elastin degradation supported selecting **1.5-minute intervals** as meaningful time points for biaxial mechanical testing. This combined analysis confirmed that full elastin removal occurred well before the 15-minute endpoint and guided the selection of degradation time interval stages for mechanical characterization.

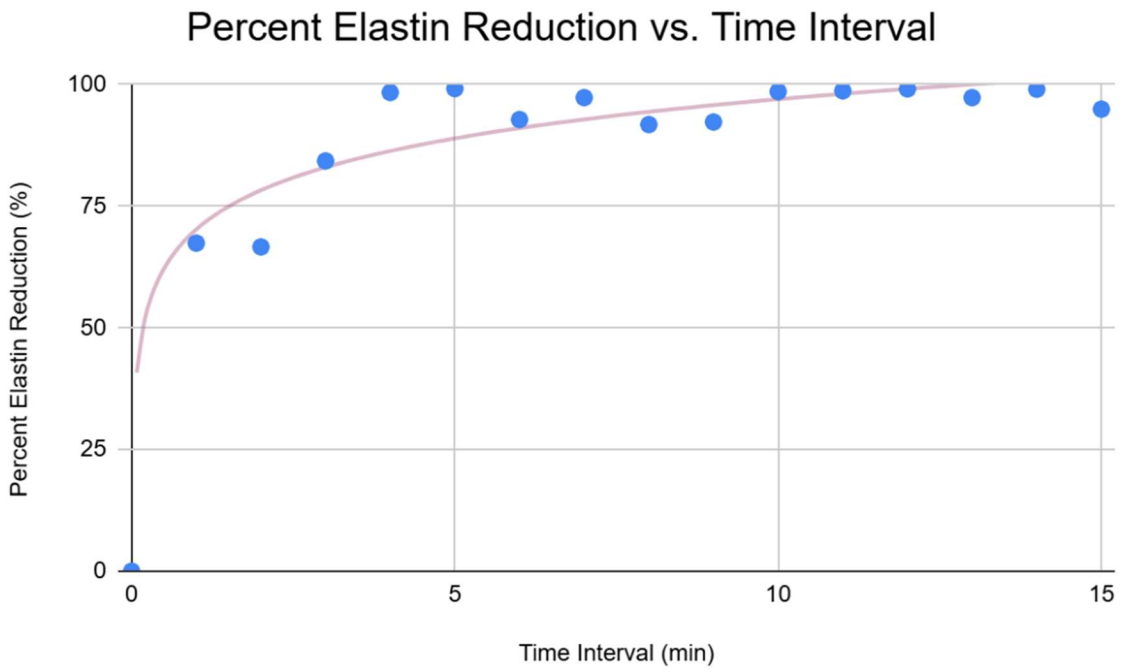

Figure 8: *Percent elastin reduction over time, showing rapid early degradation and a plateau indicating nearly complete degradation by approximately 9 minutes.*

Biaxial Mechanical Testing

Biaxial mechanical testing was performed to characterize and compare the mechanical response of the control and elastase treated MVAL tissue. A 10 × 10 mm sample was cut from the anterior leaflet and prepared for testing (Ross *et al*, 2019). Tissue thickness was measured at three locations using a Keyence laser displacement sensor, and the average value was used to calculate membrane stress. Each sample was mounted to a biaxial testing system equipped with 1.5 N load cells (BioTester, CellScale, Canada) using five tined BioRakes. The sample was oriented so that the circumferential direction aligned with the *X*-axis and the radial direction aligned with the *Y*-axis. All tests were performed in a PBS bath maintained at 37 °C to preserve physiological conditions.

Each sample underwent a standard preconditioning routine to restore its native mechanical response. Preconditioning consisted of loading the sample to a preload equal to 5 percent of the target membrane tension, followed by eight cycles up to a peak biaxial membrane tension of 150 N/ m. After preconditioning, the displacements associated with the maximum applied tension were determined for the three biaxial tension ratios: T_{circ}:T_{rad} = 1:1, 1:0.5, and 0.5:1. A displacement-controlled biaxial tensile test was then performed using these displacements, with four loading and unloading cycles at each ratio. Following the tensile test, a biaxial stress relaxation test was performed called creep. The sample was stretched to the configuration associated with the peak membrane tension T_{max} (1:1 ratio) and held at that displacement for 20 minutes. Throughout testing, a CCD camera (The Imaging Source, DMK 41AU02) captured 1280 × 960 images at 5 Hz.

After the initial mechanical test, the sample remained mounted in the device for enzymatic treatment. A 3D-printed enzyme bath containing 2 mL of the elastase mixture (phosphate buffered saline, 60 units per milliliter elastase, and 0.1 mg per milliliter trypsin inhibitor) was placed over the PBS bath (Figure 9). Both baths were maintained at 37 °C. The tissue was submerged in the enzyme solution for 1.5 minutes. At the end of the treatment period, the enzyme bath was removed, and the sample was rinsed thoroughly with 4 °C PBS to remove residual enzymes. The sample then underwent another round of preconditioning and biaxial testing using the same protocol as before.

This sequence of enzyme exposure followed by mechanical testing was repeated six additional times, giving a total of 9 minutes of progressive elastin degradation (Figure 9). Force and displacement were recorded at 5 Hz throughout the experiment to quantify how elastin removal altered stretch, stress, and overall mechanical behavior.

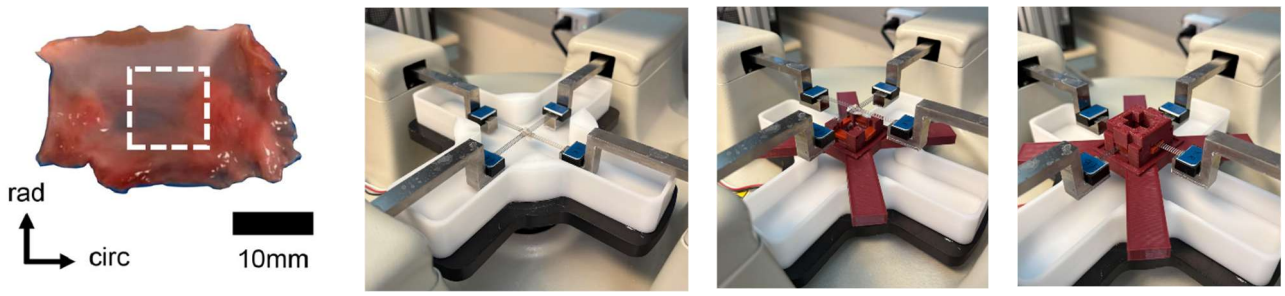

Figure 9: *A 10×10 mm MVAL sample undergoing the experimental workflow: initial PBS submersion (left), lifting to position the enzyme bath (middle), and immersion in enzyme solution for timed degradation (right).*

RESULTS

Biaxial Data – T_{circ}:T_{rad} = 1:1

Stress and stretch values were obtained from the biaxial tests to quantify how the tissue response changed with elastin degradation. Stress was calculated as force divided by the current cross-sectional area of the sample, using the measured thickness and the 10 × 10 mm testing region. Stretch was defined as the ratio of the current displacement to the initial displacement recorded at the start of loading. These two measures provided a direct way to compare how the tissue stiffened or softened under different loading conditions and across the progressive enzyme treatments.

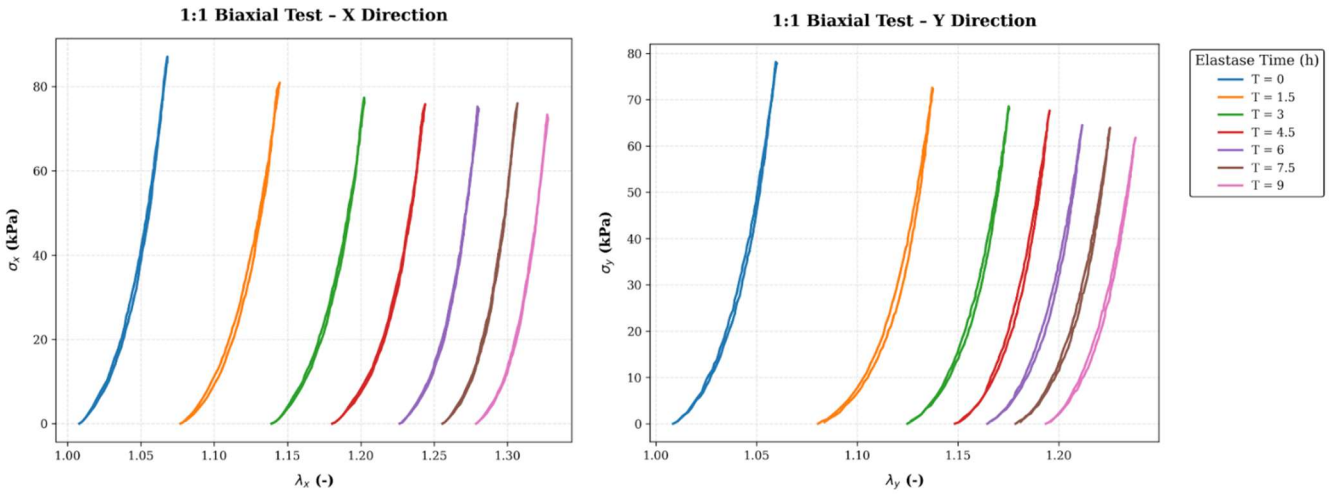

Figure 10: *Stress-stretch response in the circumferential (left) and radial (right) direction.*

Tissue Stretch

Stretch increased in both the circumferential and radial directions as elastin was removed from the tissue. Stretch was defined as the ratio of the final displacement to the initial displacement, allowing direct comparison of deformation across treatment stages. In the untreated state, the leaflet showed limited deformation because elastin provided recoil in both directions. As elastin degraded over the 9-minute treatment period, the tissue lost this recoil capability and began to deform more under similar applied loads (Figure 10). Overall, stretch increased by roughly one third compared to the untreated condition, indicating a substantial rise in compliance and a permanent set introduced by elastin loss. The increase in stretch in both the circumferential and radial directions reflect the same underlying mechanism. Without elastin, the tissue no longer returns fully to its original configuration after loading.

Tissue Mechanical Stress

Stress values decreased in both the circumferential and radial directions as elastin degradation occurred (Figure 10). Stress was calculated as force divided by the current cross-sectional area of the sample. In the untreated condition, elastin contributed significantly to load support at low and moderate strains, producing higher stresses for a given stretch in both axes. As elastin was degraded, the tissue relied more heavily on collagen fibers to carry load. Since collagen engages later in the deformation process and contributes less to low strains, the overall response declined across the 9-minute treatment period. This decrease was seen in both directions. Thus, reduction in stress demonstrates that elastin removal weakens the early strain stiffness of the leaflet and shifts the load bearing role toward a collagen dominated response.

Stored Elastic Energy Profile

The area under the stress-stretch curve, representing strain energy density, decreased in both the circumferential and radial directions as elastin was removed (Figure 10). In the untreated state, elastin allowed the leaflet to store mechanical energy through elastic recoil, producing larger areas and smaller slopes under the curve in both axes. As elastin degraded, the slope of the stress stretch curve sharpened, and the area under the curve was reduced. This reduction indicates a loss of energy storing capacity and a shift toward a more collagen-driven mechanical response. The decline was observed in both directions as well. Hence, the reduced area under the curve reflects diminished mechanical resilience and confirms that the leaflet becomes less efficient at storing energy once elastin content is reduced.

Creep Data

Another dataset collected in this study was the creep dataset (Figure 11). For this test, the tissue was brought to the target T_{circ}:T_{rad} = 1:1 loading condition and then held at a constant force for 20 minutes. Once the force level was reached, the stretch was recorded over time to see how the tissue continued to stretch while the load stayed the same. This dataset captures the time dependent behavior of the leaflet, since any increase in stretch during the hold reflects creep. Comparing the creep response before and after elastin removal showed how the loss of elastic fibers changed the long-term deformation in both the circumferential and radial directions.

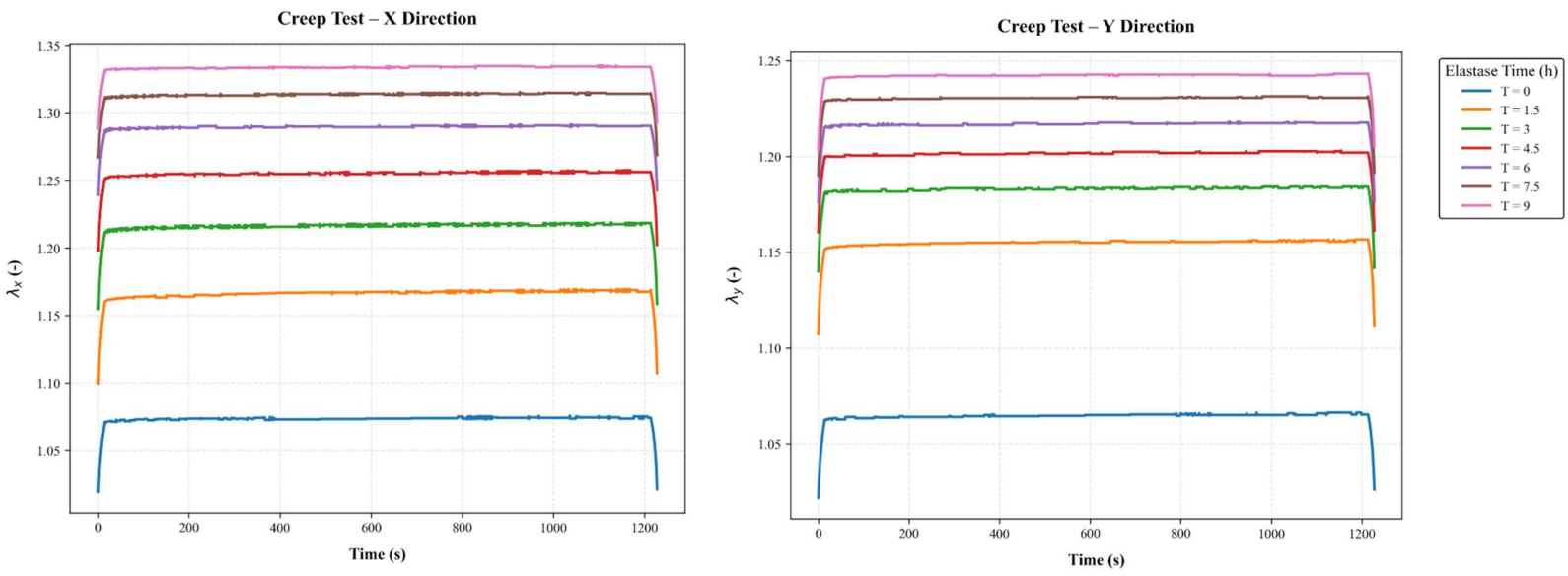

Figure 11: *Creep in the circumferential (left) and radial (right) directions under constant load.*

Stretch under Creep

Stretch increased as elastin was removed from the tissue. Since elastin provides the main source of elasticity, its loss caused the leaflet to take on a permanent stretch and show larger displacements under the same applied load. In both the circumferential and radial directions, the tissue continued to stretch once elastin was no longer resisting deformation (Figure 11). Across the 9-minute degradation period, the overall stretch increased by roughly one third compared to the untreated condition. This rise in stretch reflects the loss of elastic recoil and shows that the tissue became more compliant and less able to return to its original shape after loading.

Creep Response - The Plateau Region

The creep curves showed clear changes in the plateau region as elastin degraded. In the untreated state, the plateau had a noticeable upward angle because elastin allowed the tissue to continue stretching slowly over time while providing resistance (Figure 11). As elastin was partially removed, this angled plateau became less pronounced, indicating that the tissue was losing its ability to store elasticity during the hold period. With further degradation, the plateau flattened,

showing that the tissue no longer had stretching. This flattening of the plateau is consistent with the loss of elastin's role in long term deformation.

Collagen

Collagen fibers behave more like a strong, inelastic material similar to nylon and prevent the tissue from stretching beyond a certain point. As elastin was lost, the load shifted almost entirely to the collagen network, which restricted further elongation and defined the maximum stretch the tissue could reach (Sacks, Yoganathan 2007). This collagen-dominated response explains why the tissue maintains deformation after significant elastin removal.

DISCUSSION

The results of this study show clear and consistent changes in the mechanical behavior of the anterior mitral valve leaflet as elastin was progressively removed. Across biaxial tests, both the circumferential and radial directions demonstrated increased stretch, reduced stress, and lower strain-energy storage as the 9-minute degradation period progressed (Figure 10). These findings align with the known structural roles of elastin and collagen in soft tissues and highlight how even partial elastin loss can alter the functional mechanics of the leaflet.

Stretch values increased steadily with each round of enzymatic treatment. Because stretch was defined as the ratio of final displacement to initial displacement, this increase directly reflects the loss of elastic recoil in the tissue. Elastin normally provides early stiffness and helps the leaflet return to its original configuration after loading (Sacks, Yoganathan 2007). Once degraded, the tissue became more compliant and continued to deform under the same applied loads. This effect was observed in both the circumferential and radial directions (Figure 10). By the end of the 9-minute treatment period, the overall stretch had increased by roughly one third compared to the untreated state, indicating a permanent set and a substantial reduction in elastic resistance.

The stress response also changed. Stress, calculated as force divided by cross-sectional area, decreased as elastin was removed. In the untreated condition, elastin contributed significantly to load support at low and moderate strains, producing higher stresses for a given stretch. As elastin degraded, the tissue relied more heavily on collagen fibers, which do not engage until higher strains. This shift caused a drop in stress in both directions. The reduction in stress demonstrates that elastin plays a key role in early-strain load bearing and that its removal weakens the tissue's ability to resist deformation.

The area under the stress-stretch curve, which represents an energy density profile, also declined with elastin loss (Figure 10). In the untreated state, the leaflet stored more mechanical energy due to elastin since elastin is the energy storing protein. As degradation progressed, the slope of the curve decreased and the area under the curve became smaller, indicating reduced energy storing capability. This change was evident in both the circumferential and radial directions. The overall trend was similar where the leaflet became mechanically less efficient and more passive as elastin content reduced.

The creep dataset provided additional insight into the time dependent behavior of the tissue. When the sample was held at a constant force for 20 minutes under the T_{circ}:T_{rad} = 1:1 loading condition, the partial degraded tissue showed a gradual increase in displacement over time, reflecting viscoelastic creep (Figure 11). After elastin removal, the creep response changed slightly. The plateau region of the creep curve, which initially had an upward angle due to elastin allowing slow, controlled stretch, began to flatten as elastin degraded. This flattening indicates that the tissue lost its ability to store elastic energy during the hold period and instead deformed in a more passive, time-dependent manner. The continued increase in displacement during the hold

period further supports the conclusion that elastin loss leads to permanent stretch and reduced recoil.

Overall, the combined biaxial and creep results show that elastin plays a central role in maintaining the leaflet's elasticity, initial strain stiffness, and energy storing capacity. Its removal leads to increased compliance, reduced stress, lower energy storage, and greater time-dependent deformation. These findings highlight the importance of elastin in preserving normal valve function and provide a mechanical explanation for how elastin degradation may contribute to pathological leaflet remodeling. These results are important because they offer a clearer picture of how structural deterioration progresses in the mitral valve and how the loss of elastin alters the tissue's ability to withstand physiological loading. By identifying the mechanical effects of elastin degradation, this work improves our understanding of degenerative valve disease and helps explain why aged or diseased leaflets become more compliant and prone to long-term deformation. These insights are expected to support the development of more accurate computational models of valve mechanics and may ultimately inform more effective surgical repair strategies.

FUTURE RESEARCH DIRECTION

A natural next step for this work is to determine whether the mechanical effects of elastin loss observed here are uniform across the entire anterior mitral valve leaflet or vary by region. In this study, we focused on a single sampling location, but future experiments should compare elastin content and mechanical response in the central region and along the edge to test whether regional differences in elastin lead to different patterns of stretch, stress, and creep. Establishing these differences would provide a more complete picture of how local matrix composition shapes leaflet function. In parallel, the biaxial and creep data generated here can be used to inform and calibrate computational models of valve mechanics that are directly relevant to heart healthcare.

By integrating patient specific geometry with models that account for elastin degradation, these simulations could help predict how individual valves will respond. In the long term, such models may support the design of medical devices and repair strategies that are more customizable to each patient's valve structure and material properties, improving both durability and functional outcomes.

REFERNECES

[1] Carrabba N, Amico MA, Busi G, *et al.* The PREVASC study: Prospective Registry of Valve Disease in Asymptomatic Italian Elderly Subjects. *Aging Clin Exp Res*. 2025;37:98.

[2] Chang BS, Randall CS, Lee YS. Stabilization of lyophilized porcine pancreatic elastase. *Pharm Res*. 1993;10:1478-1483.

[3] Duca L, Amico M, Busi G, *et al.* Matrix aging and vascular impacts: focus on elastin fragmentation. *Cardiovasc Res*. 2016;110(3):298-308.

[4] Heart360Care. Understanding mitral stenosis: causes, symptoms, and advanced treatment options. *Heart360Care*. (Year not provided).

[5] Kodigepalli KM, Thatcher SE, Ghatak S, *et al.* Biology and biomechanics of the heart valve extracellular matrix. *J Cardiovasc Dev Dis*. 2020;7(4):57.

[6] Mayo Clinic Staff. Mitral valve prolapse: Symptoms and causes. *Mayo Clinic*. 2024.

[7] Rehman I, Rehman A. Anatomy, Thorax, Heart. In: *StatPearls* [Internet]. Treasure Island (FL): StatPearls Publishing; 2026 Jan. Updated 2023 Aug 28.

[8] Ross CJ, Bersi MR, Hsu EW, *et al.* An investigation of the glycosaminoglycan contribution to biaxial mechanical behaviors of porcine atrioventricular heart valve leaflets. *J R Soc Interface*. 2019;16(156):20190249.

[9] Ross CJ, Bersi MR, Hsu EW, *et al.* Effects of enzyme-based removal of collagen and elastin constituents on the biaxial mechanical responses of porcine atrioventricular heart valve anterior leaflets. *Acta Biomater*. 2021;135:425-440.

[10] Sacks MS, Yoganathan AP. Heart valve function: a biomechanical perspective. *Philos Trans R Soc Lond B Biol Sci*. 2007;362(1484):1369-1391.